NATIONAL TRANSPORTATION SAFETY BOARD
Office of Aviation Safety
Aviation Engineering Division
Washington, DC 20594

December 5, 2003

ADDENDUM NUMBER 2 TO THE STRUCTURES GROUP CHAIRMAN'S FACTUAL REPORT

DCA02MA001

A. ACCIDENT

Location:	Belle Harbor, NY
Date:	November 12, 2001
Time:	09:16:14 EST
Aircraft:	American Airlines Flight 587, Airbus Model A300-605R, N14053 Manufactures Serial Number (MSN) 420

B. STRUCTURES GROUP

Chairman: Brian K Murphy
National Transportation Safety Board
Washington, DC

C. AIRBUS REPORT

1. ***"AAL587 Investigation, Accident Analysis – FEM Global model VTP & Rudder"***

AIRBUS

Technical Note

Report Nr.: TN – ESGC – 1017/03

Author:
Department.:

Title

AAL587 Airbus Structure Investigation

Accident Analysis - FEM Global model - VTP & Rudder

Date: 08.12.2003

Summary:

For the investigation of the loading conditions sustained by the vertical stabilizer during the accident of flight AAL587 a detailed 2D FEA-model has been created for the fin box, the rudder and the rudder supports.

The report describes the idealization of the model and the analysis performed. Results are provided in terms of strains, displacements and attachment forces.

The FEA with the last two peak loading conditions during the accident was compared with the limit load condition of the design lateral gust case. The analysis (W375 loading condition) revealed a limit load factor of 2.05 for the resultant attachment force at the RHS rear lug and the max. strain level in the skin panel relative to the lateral design gust case (BI17) of the A300-600R. The variation of the fuselage stiffness (static over determined) shows for realistic changes no significant influence. The hinge line forces for load case W375 are not at a level to cause a failure of the rudder support structure.

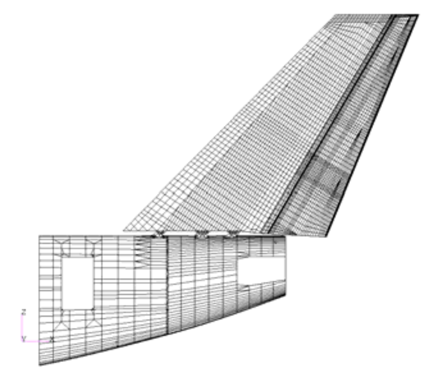

Public Docket	Issue	Date	No. of page	Revised pages	Valid from/for
	1	10.11.2003	28		
	2	02.12.2003	28	Format change DINA4 to LETTER	
	3	08.12.2003	28		

Table of contents

1. Introduction

For the investigation of the loading conditions sustained by the vertical stabilizer during the accident of flight AAL587 a detailed 2D FEA-model has been created for the fin box, the rudder and the rudder supports.
This model is attached to the rear fuselage which is clamped far enough from the fin attachment to avoid structural interference.
The report describes the idealization of the model and the analysis performed. Results are provided for

- the design lateral gust load case BI17 for the A300-600R
- the accident loading condition W372

and

- the accident loading condition W375

in terms of strains, max. fin deformation and attachment forces.

The influence of the rear fuselage stiffness on the fin attachment loads between front, center and rear fittings has been discussed.

2. Global 2D-FE-model for vertical stabilizer and rudder structural analysis

2.1 Detailed view of the A300-600R VTP structure components

The main structure components of the vertical stabilizer are shown on figure 2.1. The fin box itself is assembled from front spar, center spar, rear spar, LHS and RHS skin panels and 18 ribs as shown on figure 2.2.

Components of the VTP

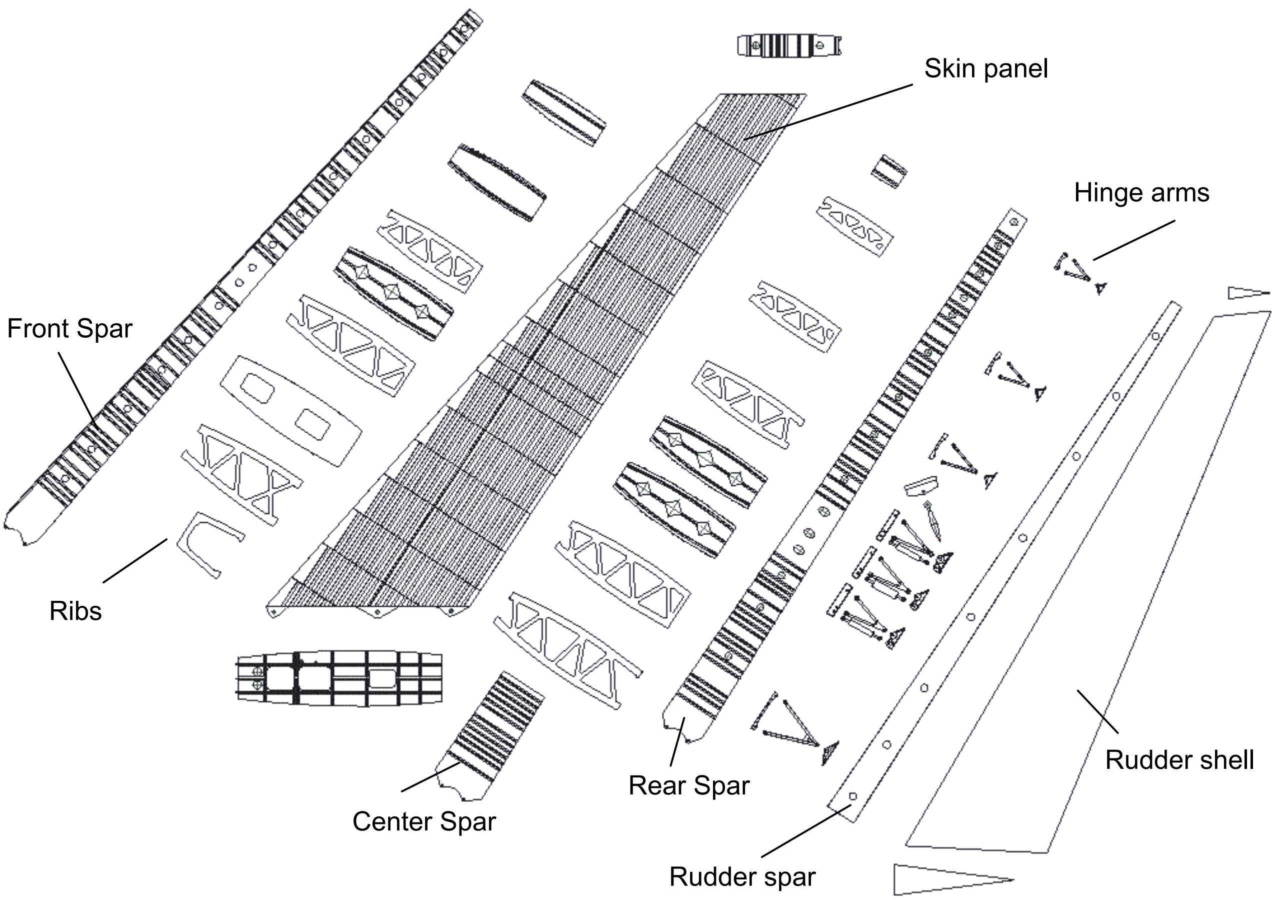

Figure 2.1

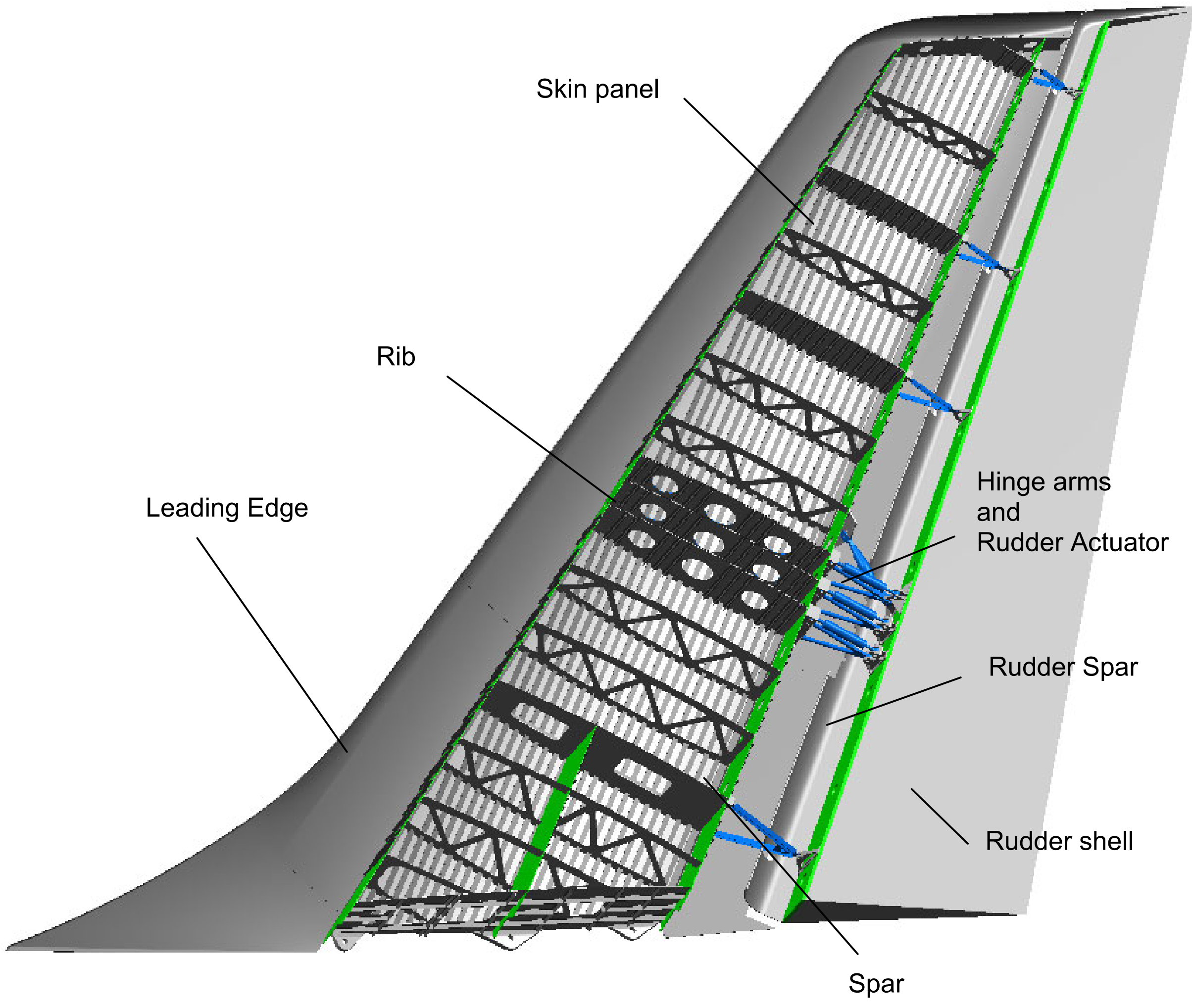
Skin panel
Rib
Leading Edge
Hinge arms
and
Rudder Actuator
Rudder Spar
Rudder shell
Spar

Figure 2.2

2.2 FEA-model used for the AAL587 accident investigation

The FEA-model used for the AAL587 accident investigation is based on the certification model from 1985. See figures 2.3 to 2.5.

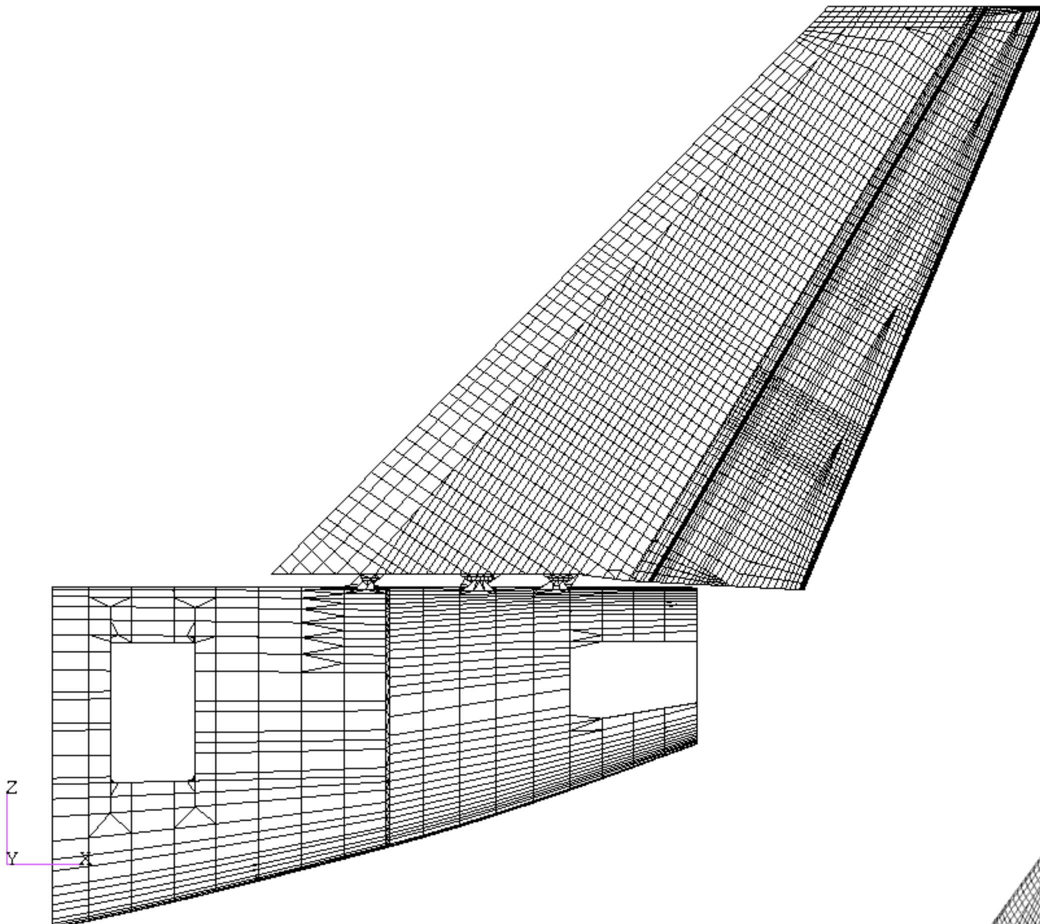

Figure 2.3

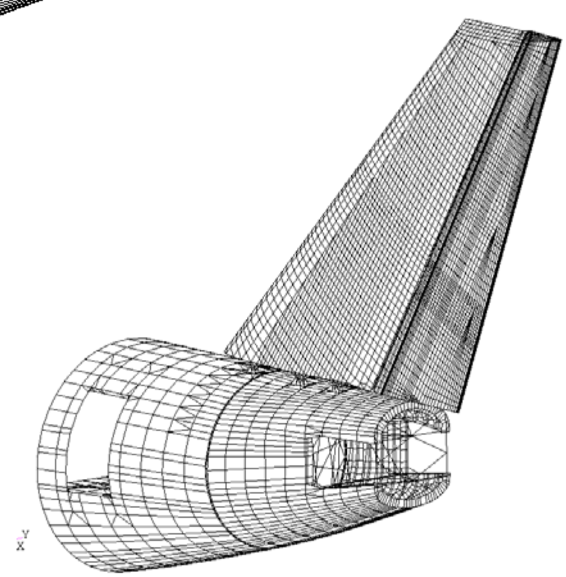

Figure 2.4

In addition to the original justification model from 1985 the following structure components are included in the new model according.

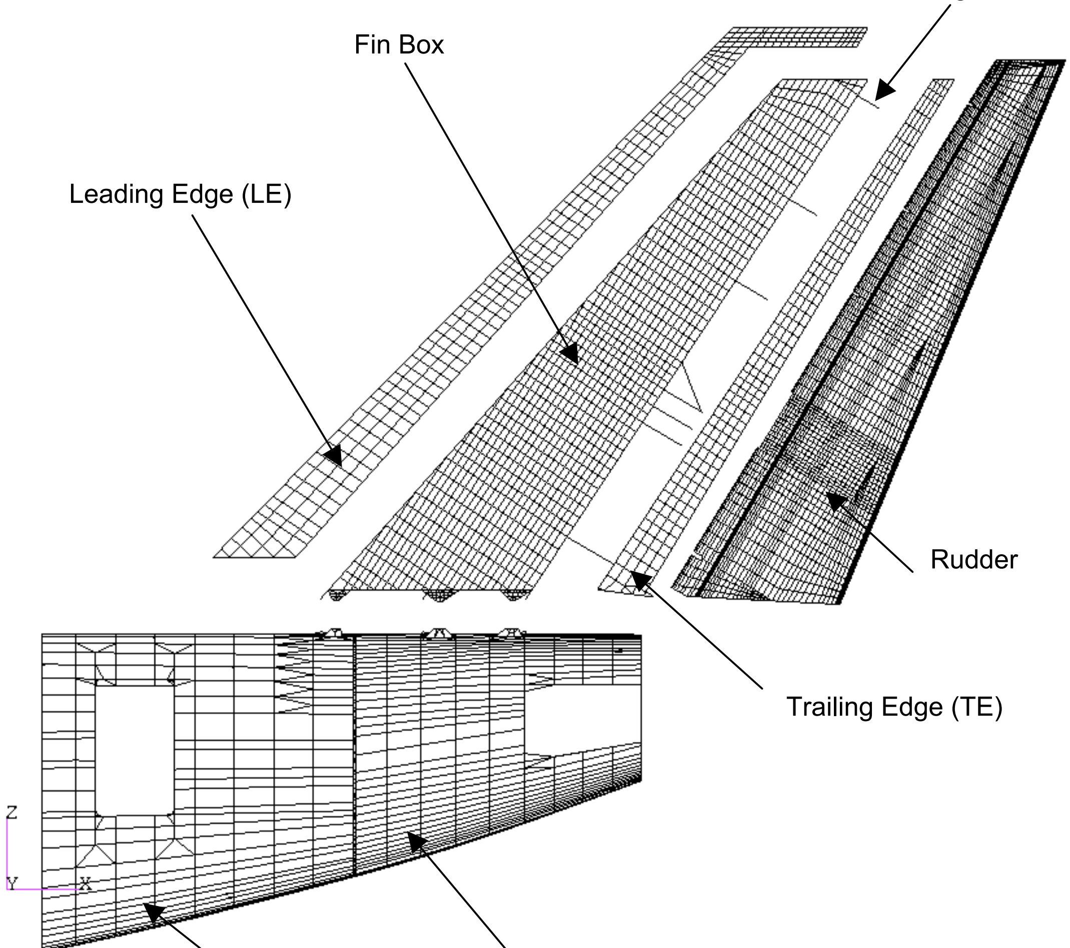

Figure 2.5

2.3 Idealization of the skin panel

The ply stacking of the skin was modeled with MAT2 material cards and PSHELL elements.

In the certification model the skin field between 2 ribs and 2 stringers was modeled with one quadrilateral element each. For the accident investigation model it was decided to remesh these areas with four elements instead of one, to achieve a more detailed strain distribution information for the skin panels. See following figures 2.6 to 2.9.

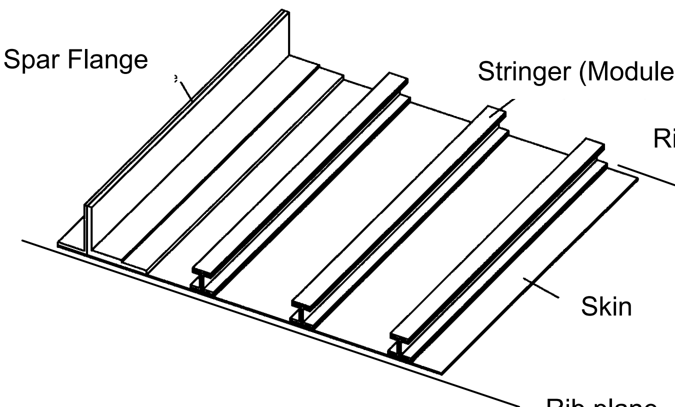

Figure 2.6

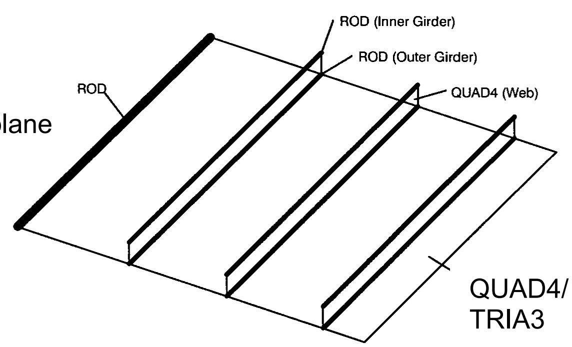

Figure 2.7

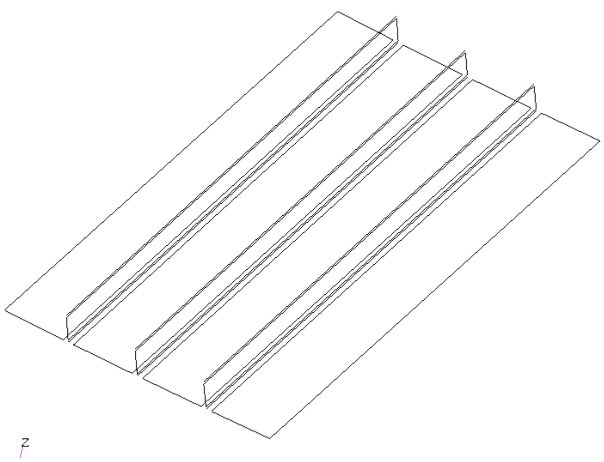

Certification model from 1985

Figure 2.8

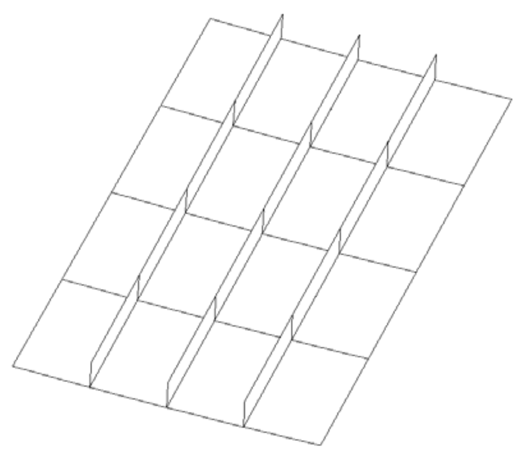

Investigation model

Figure 2.9

2.4 Idealization of the main attachment fittings

In the investigation model used properties for the lug are the same compared to the certification model from 1985.

Changes relative to the certification model from 1985 are as follows:

- use for the lug the CQUAD4 elements where possible
- lug plane is parallel to fin box center plane

Figure 2.10 shows the main attachment shape and figure 2.11 shows the corresponding FE-mesh of the investigation model.

Drawing

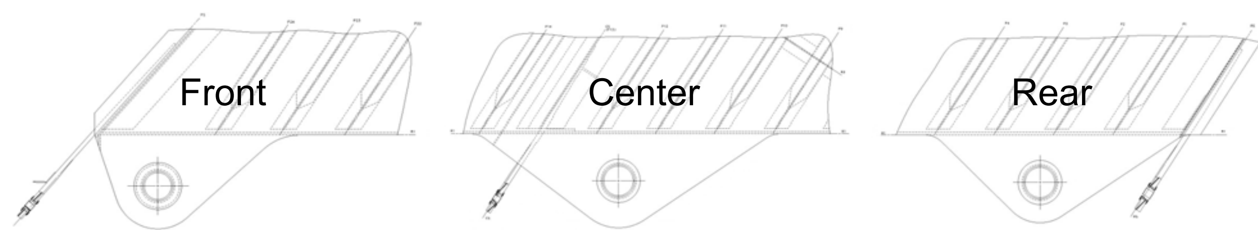

Figure 2.10

Investigation model

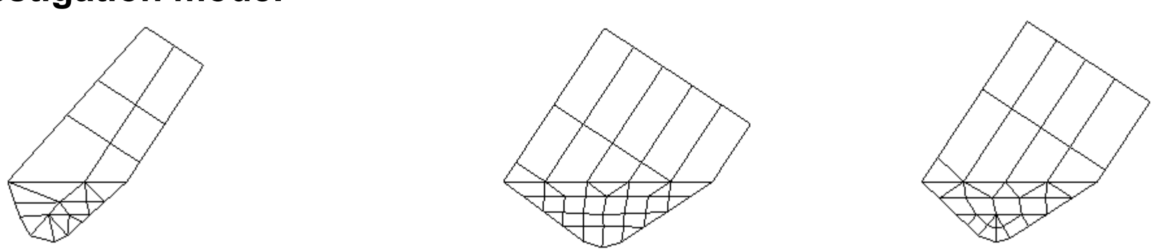

Figure 2.11

2.5 Idealization of Fuselage / VTP connection in the global 2D model

The idealization of the fuselage / VTP connection bolt in the global 2D NASTRAN model was made with two RBE2 elements (rigid body element) per fuselage clevis (see figure 2.12). One 3-node RBE2-element represented the stiff bolt in the fuselage clevis. The other RBE2-element was on the one side connected with the node of the bolt RBE2-element and on the other side, but same location, with the VTP main attachment lug center point.

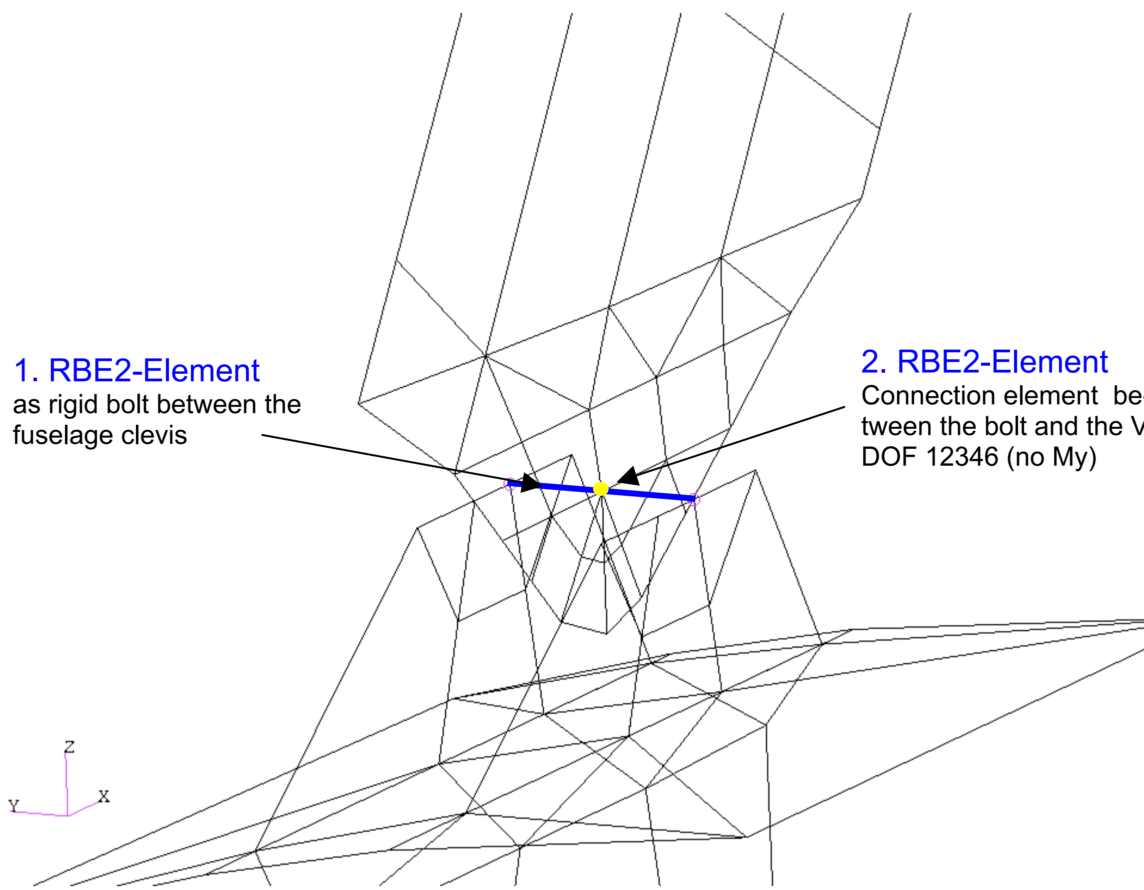

Figure 2.12

2.6 Rudder Attachment Fittings

During the analysis the behavior of the rudder attachment fittings was investigated (see figure 2.13).
To get detailed results of the attachments fittings and the attachment bolts forces, they were modeled in detail (see figure 2.14).

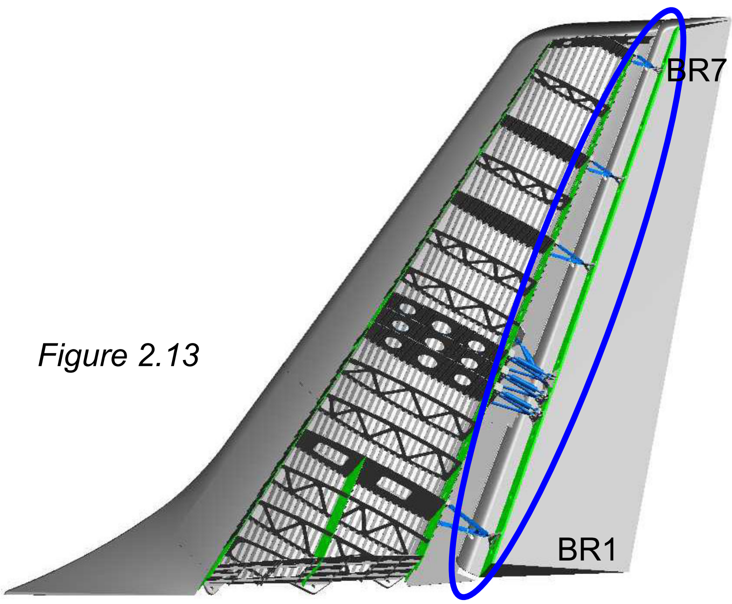

Figure 2.13

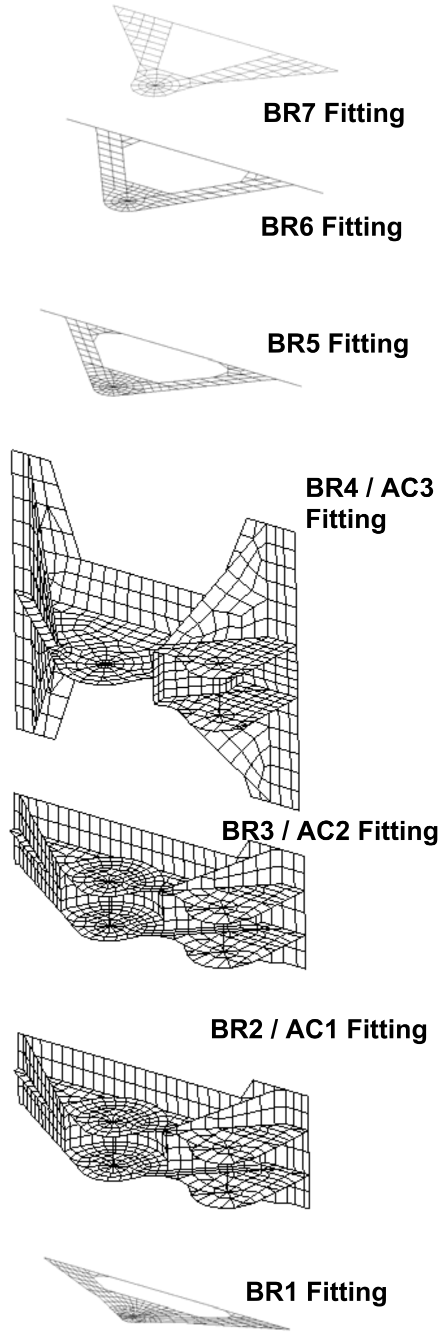

Figure 2.14

2.7 Rudder Hinge Line / Rudder Deflection

Each calculated load case (lateral maneuver) is defined by the load distribution of fin and rudder and the rudder deflection angle (see figure 2.15 and 2.16).
All analyzed load cases were calculated with the rudder in deflected position.

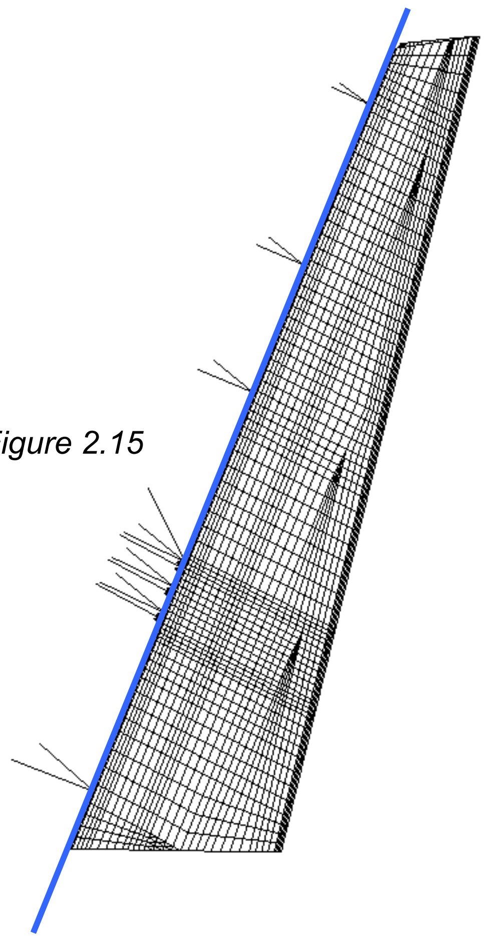

Figure 2.15

Rudder hinge line at 70% of the VTP chord length

Rudder deflection sign convention

A positive rudder deflection angle means rudder trailing edge to the left.

A negative rudder deflection angle, means rudder trailing edge to the right.

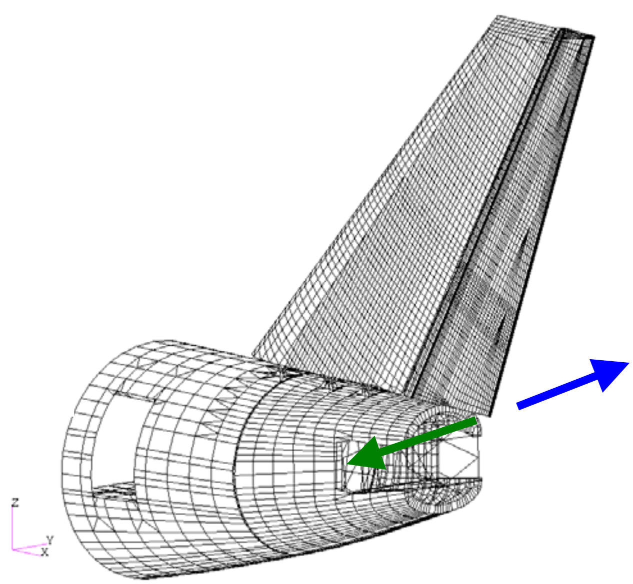

Figure 2.16

2.8 Boundary Conditions of the global model

The structural model is clamped (Degree of Freedom 1-6 /translation and rotation) at the perimeter of the first frame C72 of section 18 (see figure 2.17).

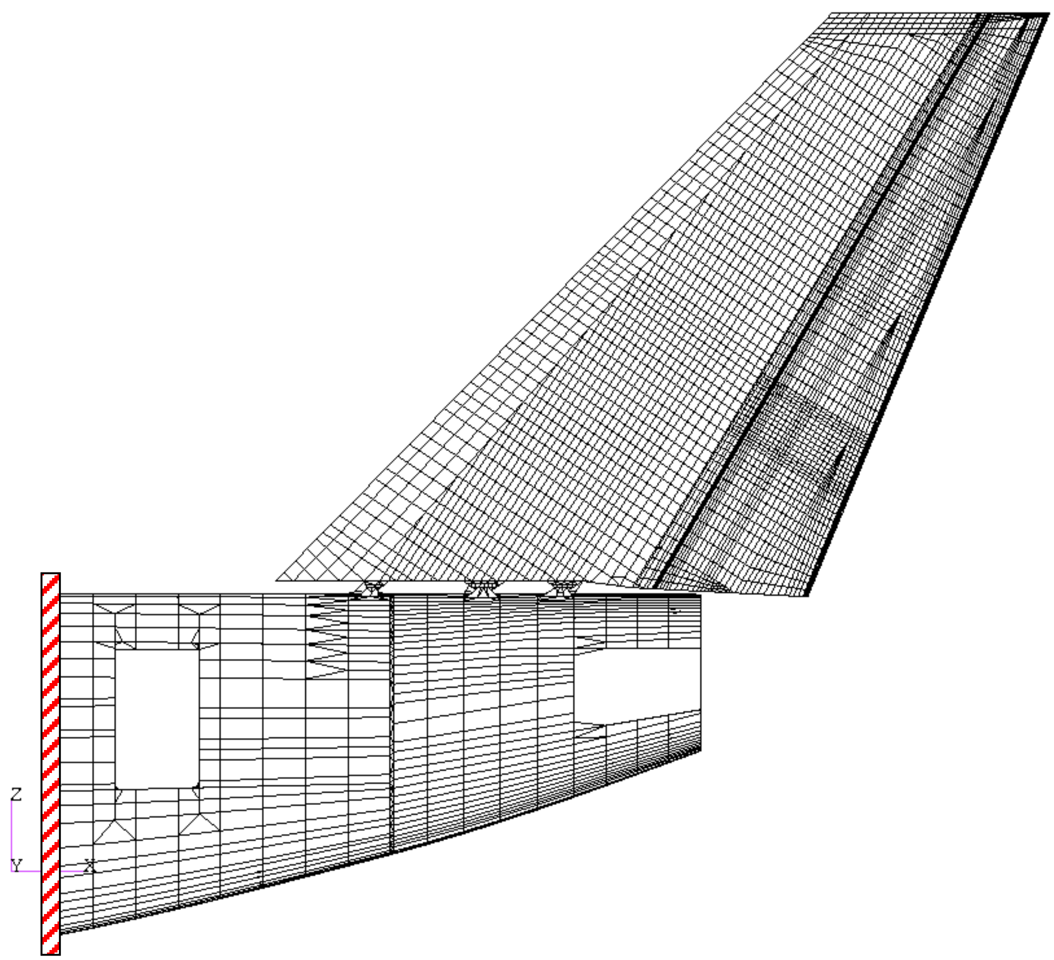

Figure 2.17

3. Description of considered load cases

The loads are provided as nodal forces on both surfaces of the finite element model. The load resultants Qy, Mx and Mz are given in the global coordinate system or in the fin coordinate system which is defined by the 36.5% chordline of the vertical stabilizer. The origin of these coordinate systems is the intersection with the global system X-axis which is 85mm below the fin box main fitting center line (see figure 3.1).

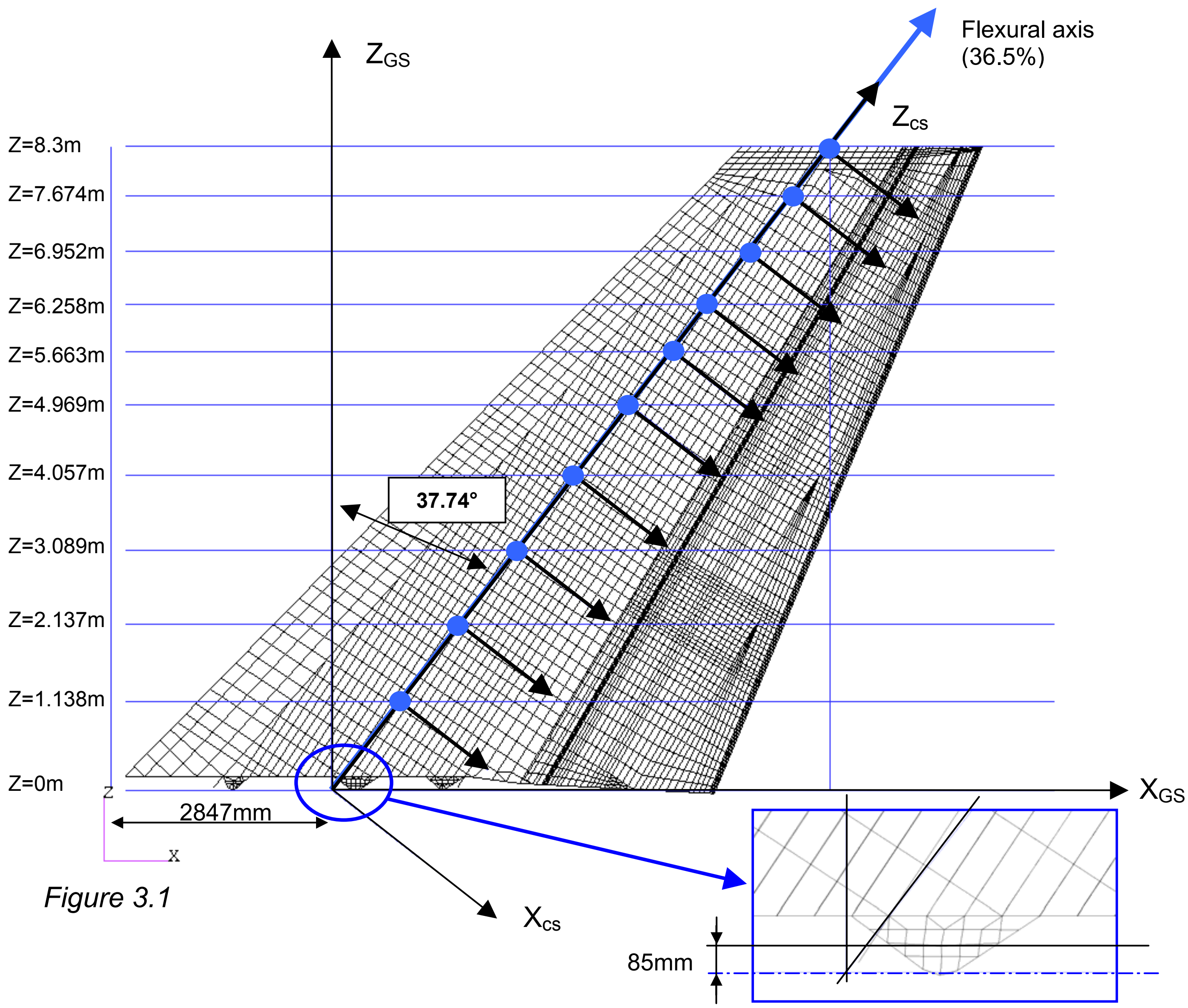

Figure 3.1

GS	**G**lobal coordinate **S**ystem
CS	VTP **C**omponent coordinate **S**ystem / flexural axis aligned

The lateral force is for both systems the same, but the moment Mx and Mz have to be transformed. The relationship of the moments between these two coordinate system is given by the equations below.

<u>Global Coordinate System to Component Coordinate System</u>

$$Mz_{cs} = Mx_{gs} \cdot \sin\alpha + Mz_{gs} \cdot \cos\alpha$$ $\alpha = 37.74°$ (see figure 3.1)

$$Mx_{cs} = Mx_{gs} \cdot \cos\alpha - Mz_{gs} \cdot \sin\alpha$$

<u>Component Coordinate System to Global Coordinate System</u>

$$Mz_{gs} = -Mx_{cs} \cdot \sin\alpha + Mz_{cs} \cdot \cos\alpha$$

$$Mx_{gs} = Mx_{cs} \cdot \cos\alpha + Mz_{cs} \cdot \sin\alpha$$

4. 2D global NASTRAN VTP model results

4.1 Design lateral gust load case BI17 [Limit Load]

4.1.1 Main attachment fitting forces [BI17 / Limit Load]

Table 4.1 **Load resultant at fin root** [Component System]

Load case		BI17 L.L.
Qy	[N]	-212 060
Mx	[Nm]	866 390
Mz	[Nm]	153 030

Table 4.2 **Main Fitting Reaction Forces**

Load	Front [N]		Centre [N]		Rear [N]	
component	LHS	RHS	LHS	RHS	LHS	RHS
Fx	134392	-133432	105747	-107032	178043	-177638
Fy	8392	8429	19324	19451	21014	21317
Fz	186089	-186552	365710	-364532	433075	-433669
Fres	**229697**	**229514**	**381181**	**380418**	**468716**	**469125**
Mx [Nm]	-1806	-1804	-4193	-4221	-5485	-5438
Mz [Nm]	21	27	510	458	2009	1948
angle [°]	54	54	74	74	68	68

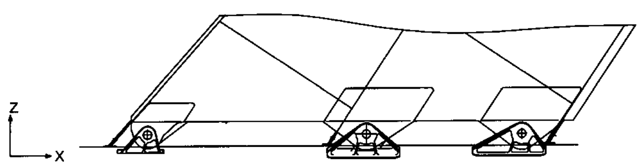

Figure 4.1

Table 4.3 **Lateral Load Yokes Reaction Forces**

Load	Front [N]		Centre [N]		Rear [N]	
component	LHS	RHS	LHS	RHS	LHS	RHS
Fx	-1262	1261	-792	754	-3613	3573
Fy	16987	16970	10828	10310	29685	29356
Fz	-1437	1435	-1207	1149	-5513	5452
Fres	**17094**	**17077**	**10923**	**10401**	**30408**	**30071**

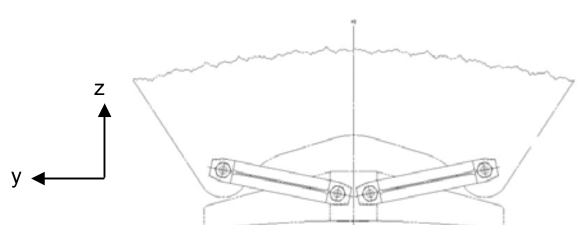

Figure 4.2

4.1.2 Fin Deformation [BI17 / Limit Load]

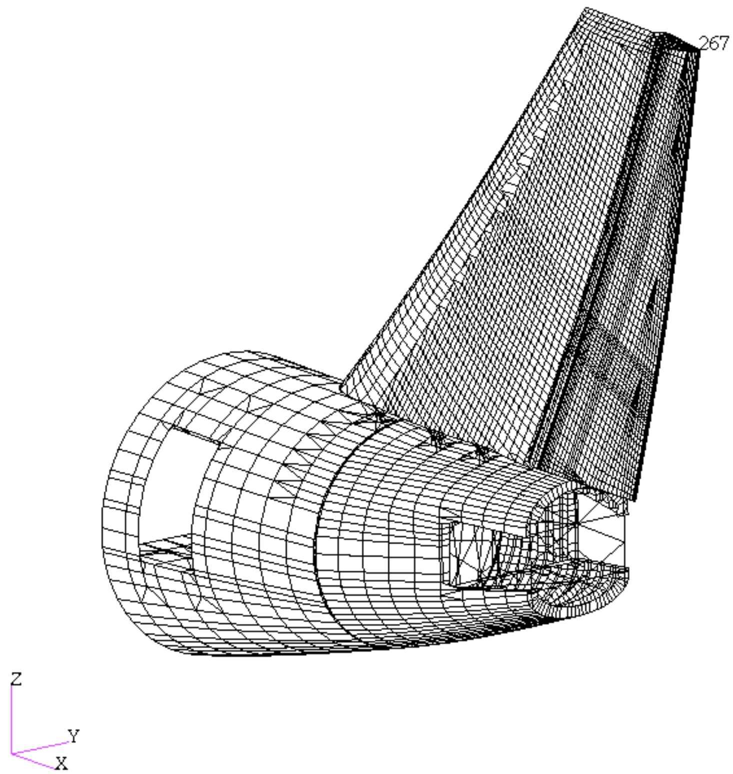

Max. fin deformation at the rudder trailing edge is 267 mm.

Figure 4.3

Deformations are scaled up for a better understanding of the structural behaviour!

4.2 Accident loading condition W372 [Ny integration issue18– Criteria: correlated corner bending Mx/torsion]

4.2.1 Main attachment fitting forces [W372]

Table 4.4 **Load resultant at fin root** [Component System]

Load case		W372
Qy	[N]	-396 160
Mx	[Nm]	1 788 750
Mz	[Nm]	86 210

Table 4.5 **Main Fitting Reaction Forces**

Load	Front [N]		Centre [N]		Rear [N]	
component	**LHS**	**RHS**	**LHS**	**RHS**	**LHS**	**RHS**
Fx	255557	-268101	240105	-244797	407194	-399366
Fy	11377	11987	35371	35863	46253	46045
Fz	308991	-326355	678450	-679268	865736	-842293
Fres	**401141**	**422527**	**720553**	**722922**	**957833**	**933311**
Mx [Nm]	-2934	-3021	-7703	-7805	-10782	-10530
Mz [Nm]	60	35	1095	1002	4274	4041
angle [°]	50	51	71	70	65	65

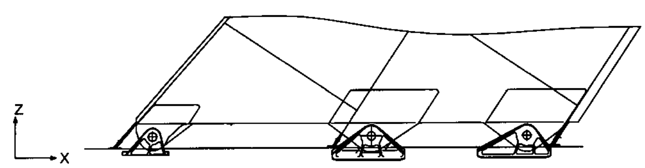

Figure 4.4

Table 4.6 **Lateral Load Yokes Reaction Forces**

Load	Front [N]		Centre [N]		Rear [N]	
component	**LHS**	**RHS**	**LHS**	**RHS**	**LHS**	**RHS**
Fx	-1262	1261	-792	754	-3613	3573
Fy	16987	16970	10828	10310	29685	29356
Fz	-1437	1435	-1207	1149	-5513	5452
Fres	**17094**	**17077**	**10923**	**10401**	**30408**	**30071**

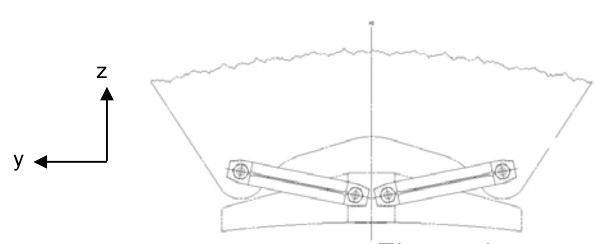

Figure 4.5

4.2.2 Hinge arm and rudder actuator forces [W372]

Rudder deflection angle	[°]	-11,47

Table 4.7 **Actio forces at the rudder attachment fitting**

	Fx [N]	Fy[N]	Fres[N]
BR1	-12095	1496	**12187**
BR2	-40605	10423	**41921**
AC1	40645	3272	**40777**
BR3	-39248	8101	**40075**
AC2	42880	3529	**43025**
BR4+Z-Force	-44929	7876	**45614**
AC3	52460	4564	**52659**
BR5	-2321	5037	**5546**
BR6	-3892	5116	**6428**
BR7	-3677	3722	**5232**

Table 4.8 **Load resultant for the rudder**

Qy Rudder	[N]	-53 140
Rudder hinge moment	[Nm]	19 290

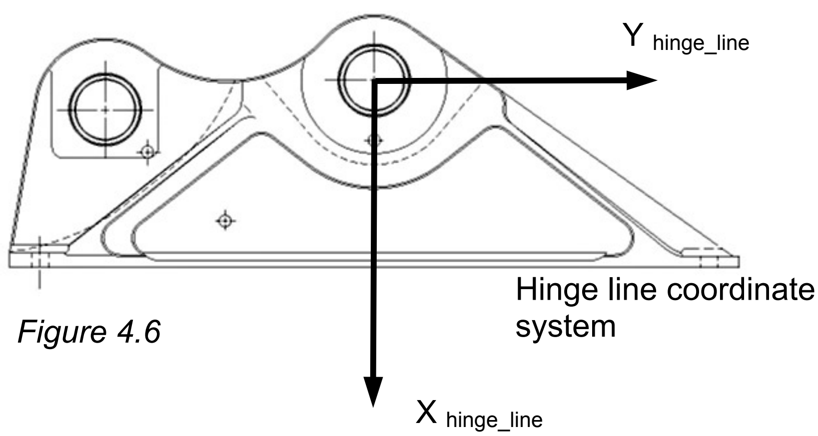

Figure 4.6

4.2.3 Rudder attachment fitting bolt forces [W372]

Table 4.9

BR1	Fx [N]	Fy [N]	Fz[N]
LHS	6646	-4576	-118
RHS	4910	704	117
BR2/AC1			
LHS	-12630	-10132	-332
RHS	9684	203	943
BR3/AC2			
LHS	-15914	-9602	-319
RHS	9849	707	102
BR4/AC3			
LHS	-22063	-11100	1369
RHS	12055	702	-1422
BR5			
LHS	2535	-3488	-1
RHS	-1262	-1909	0
BR6			
LHS	3858	-3251	-10
Mid	16	-571	24
RHS	-1077	-1966	-14
BR7			
LHS	3921	-2586	-7
RHS	-1057	-1794	6

Bolt forces are listed in the rudder spar aligned coordinate system.

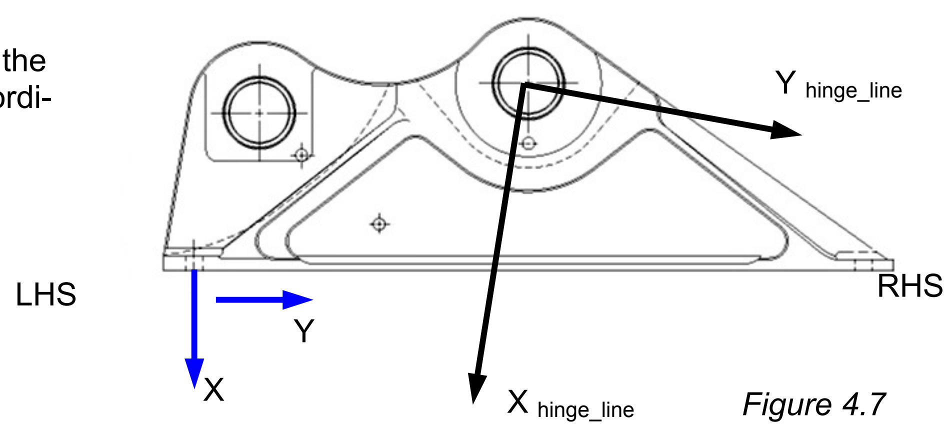

Figure 4.7

4.3. Accident loading condition W375 [Ny integration issue18– Criteria: maximum lateral acceleration Ny]

4.3.1 Main attachment fitting forces [W375]

Table 4.10 **Load resultant at fin root** [Component System]

Load case		W375
Qy	[N]	-408 470
Mx	[Nm]	1 839 970
Mz	[Nm]	94 430

Table 4.11 **Main Fitting Reaction Forces**

Load	Front [N]		Centre [N]		Rear [N]	
component	LHS	RHS	LHS	RHS	LHS	RHS
Fx	263107	-275943	246445	-251278	418158	-410119
Fy	11804	12430	36462	36969	47522	47303
Fz	319585	-337407	699593	-700429	891536	-867491
Fres	**414125**	**436054**	**742627**	**745056**	**985876**	**960716**
Mx [Nm]	-3043	-3133	-7942	-8048	-11103	-10847
Mz [Nm]	63	38	1125	1029	4397	4157
angle [°]	51	51	71	70	65	65

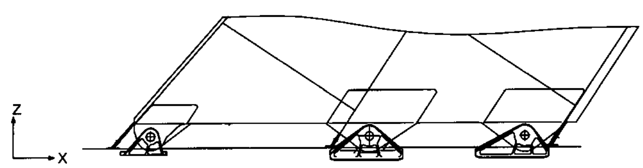

Figure 4.8

Table 4.12 **Lateral Load Yokes Reaction Forces**

Load	Front [N]		Centre [N]		Rear [N]	
component	LHS	RHS	LHS	RHS	LHS	RHS
Fx	-1245	1176	-708	599	-9868	10142
Fy	16756	15837	9681	8191	81072	83328
Fz	-1417	1339	-1079	913	-15056	15475
Fres	**16862**	**15937**	**9767**	**8264**	**83046**	**85358**

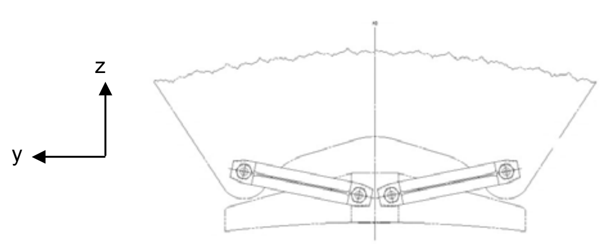

Figure 4.9

4.3.2 Hinge arm and rudder actuator forces [W375]

Rudder deflection angle	[°]	-11,47

Table 4.13 **Actio forces at the rudder attachment fitting**

	Fx [N]	Fy[N]	Fres[N]
BR1	-12430	1406	**12509**
BR2	-42021	10649	**43349**
AC1	42082	3387	**42218**
BR3	-40653	8264	**41484**
AC2	44400	3654	**44550**
BR4+Z-Force	-46575	8032	**47263**
AC3	54349	4728	**54554**
BR5	-2392	5160	**5687**
BR6	-4019	5287	**6641**
BR7	-3780	3831	**5382**

Table 4.14 **Load resultant for the rudder**

Qy Rudder	[N]	-54 400
Rudder hinge moment	[Nm]	19 980

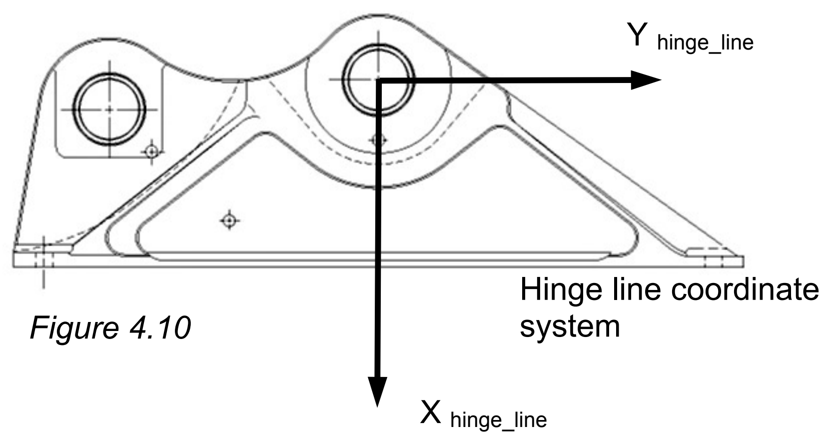

Figure 4.10

4.3.3 Rudder attachment fitting bolt forces [W375]

Table 4.15

BR1	Fx [N]	Fy [N]	Fz[N]
LHS	6814	-4636	-120
RHS	5088	787	119
BR2/AC1			
LHS	-13111	-10405	-337
RHS	10071	249	970
BR3/AC2			
LHS	-16492	-9863	-331
RHS	10249	776	106
BR4/AC3			
LHS	-22868	-11404	1377
RHS	12553	760	-1433
BR5			
LHS	2605	-3577	-1
RHS	-1287	-1956	0
BR6			
LHS	3984	-3354	-10
Mid	17	-591	25
RHS	-1114	-2034	-15
BR7			
LHS	4032	-2658	-7
RHS	-1090	-1848	7

Bolt forces are listed in the rudder spar aligned coordinate system.

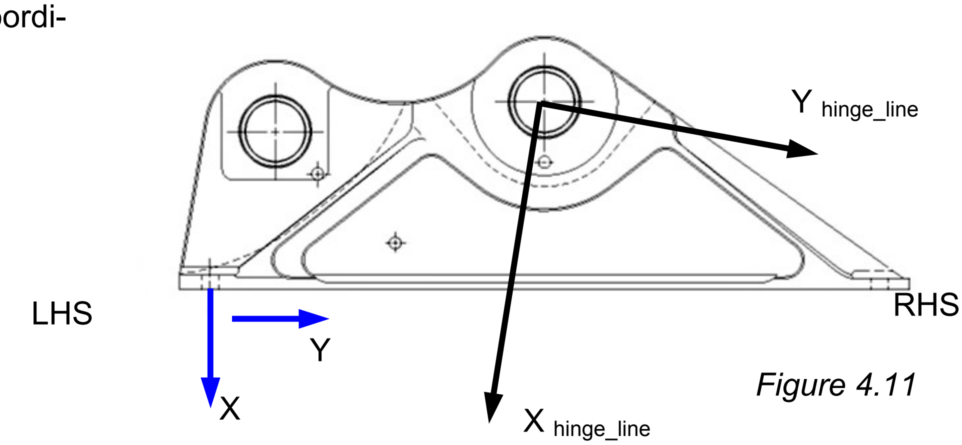

Figure 4.11

4.3.4 Fin Deformation [W375]

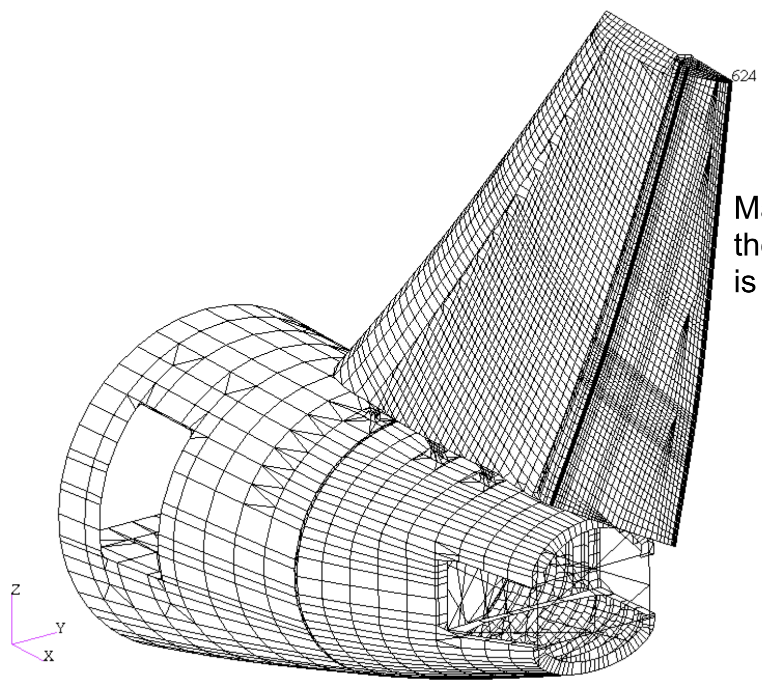

Max. fin deformation at the rudder trailing edge is 624 mm

Figure 4.12

Deformations are scaled up for a better understanding of the structural behaviour!

4.4 Influence of the rear fuselage stiffness on fin attachment loads between front, center, and rear fittings

The global force and moments distribution at the fuselage / VTP attachments depends on the stiffness distribution of both parts. A stiffness variation on the fuselage side should show the influence on the attachment force distribution (see figure 4.13). The reference model for this investigation is the original fuselage model "*Basis 1*". Based on this model a second model "*Model2*" was created with an overall fuselage stiffness increase of 10%. The third model "*Model3*" includes a 10% increased fuselage stiffness from behind the front main attachment to the aft. The last model "*Model4*" includes a 10% increased fuselage stiffness from behind the center main attachment to the aft.

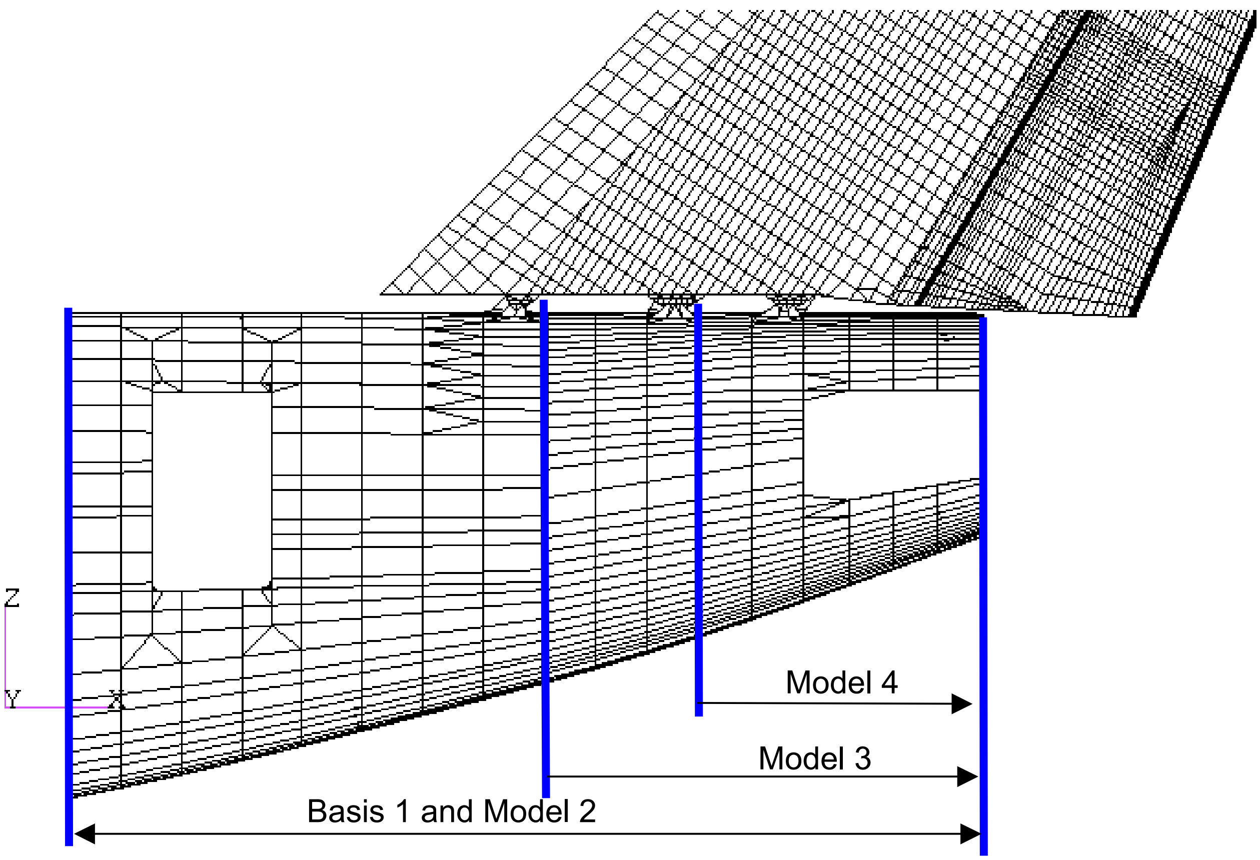

Figure 4.13

Table 4.16

Model	**Description**
Basis 1	original fuselage stiffness
Model 2	all fuselage properties Young's-modulus increased by 10%
Model 3	fuselage from front main fitting to the aft all fuselage properties Young's modulus increased by 10%
Model 4	fuselage from center main fitting to the aft all fuselage properties Young's modulus increased by 10%

The next two diagrams 4.1 and 4.2 show the changes in the resultant main fitting forces and for the lateral load yoke between the different model assumptions.

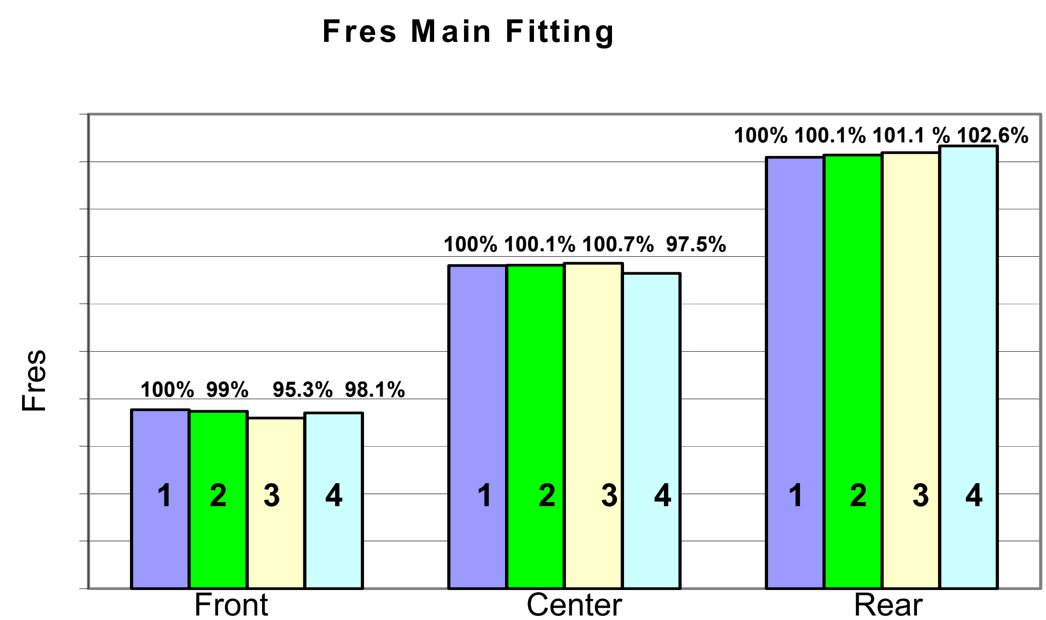

Diagram 4.1

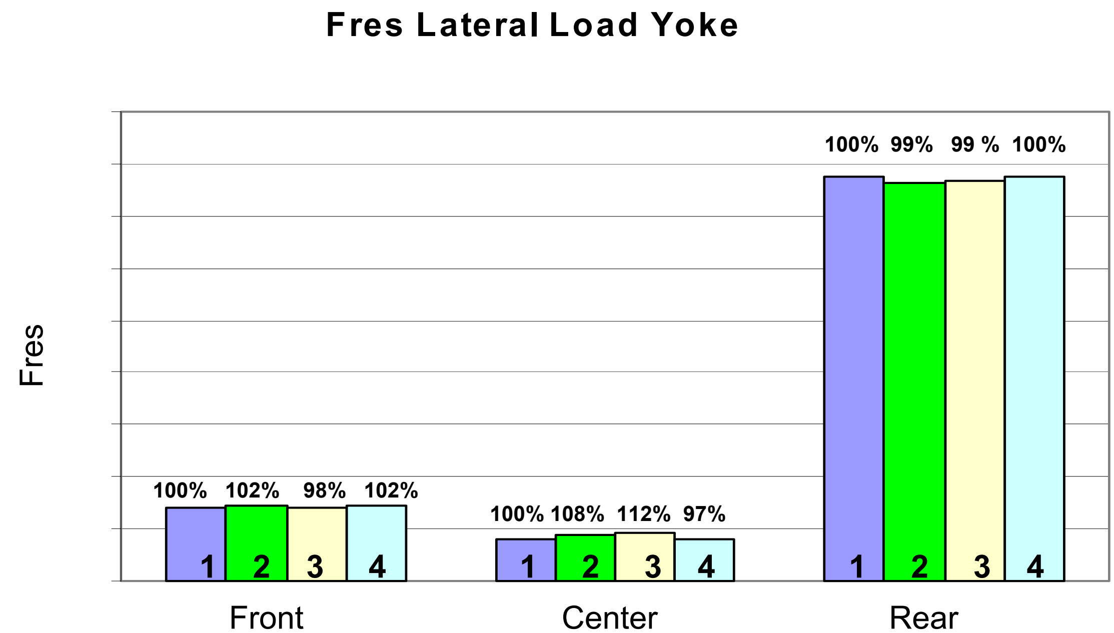
Fres Lateral Load Yoke
Fres
100% 102% 98% 102%
100% 108% 112% 97%
100% 99% 99 % 100%
1 2 3 4
1 2 3 4
1 2 3 4
Front
Center
Rear

Diagram 4.2

5. Summary

The FEA with the last two peak loading conditions during the accident was compared with the limit load condition of the design lateral gust case. The analysis (W375 loading condition) revealed a limit load factor of 2.05 for the resultant attachment force at the RHS rear lug and the max. strain level in the skin panel relative to the design lateral gust case BI17 of the A300-600R. The variation of the fuselage stiffness (static over determined) shows for realistic stiffness changes no significant influence.
The hinge line forces for load case W375 are not at a level to cause a failure of the rudder support structure.